nature chemistry

ARTICLES

PUBLISHED ONLINE: 18 MARCH 2012 | DOI: 10.1038/NCHEM.1295

Reversible hydrogen storage using CO_2 and a proton-switchable iridium catalyst in aqueous media under mild temperatures and pressures

Jonathan F. Hull[1]*, Yuichiro Himeda[2]*, Wan-Hui Wang[2], Brian Hashiguchi[3], Roy Periana[3], David J. Szalda[4], James T. Muckerman[1] and Etsuko Fujita[1]*

Green plants convert CO_2 to sugar for energy storage via photosynthesis. We report a novel catalyst that uses CO_2 and hydrogen to store energy in formic acid. Using a homogeneous iridium catalyst with a proton-responsive ligand, we show the first reversible and recyclable hydrogen storage system that operates under mild conditions using CO_2, formate and formic acid. This system is energy-efficient and green because it operates near ambient conditions, uses water as a solvent, produces high-pressure CO-free hydrogen, and uses pH to control hydrogen production or consumption. The extraordinary and switchable catalytic activity is attributed to the multifunctional ligand, which acts as a proton-relay and strong π-donor, and is rationalized by theoretical and experimental studies.

The efficient and catalytic reduction of CO_2 by photosynthesis has inspired many sustainable energy and 'clean tech' applications[1–8], because CO_2 is cheap, abundant and stable. CO_2 is also a greenhouse gas, and its fixation as part of a carbon-neutral energy cycle would significantly decrease its associated environmental risks[9]. Dihydrogen (H_2) is desirable as a fuel, because it can be converted efficiently to energy without producing toxic products or greenhouse gases, and the rates and efficiencies with which it can be obtained from water with sunlight continue to increase[10,11]. However, on an industrial scale, H_2 is constrained by its physical properties, leading to safety concerns, transport problems and a low energy density[4]. Conventional research on H_2 storage devices such as high-pressure and cryogenic gas containers is unlikely to overcome these problems, and the results have not proved economically viable[12]. Other approaches using new materials such as metal hydrides and metal organic frameworks have also been investigated, but these are limited by their high activation energy and low energy density[13]. In contrast, liquids with a high (>4%) hydrogen content can be safe to handle, offer greater energy density, and can be transported easily using the existing infrastructure for gasoline and oil. Aqueous formic acid (HCO_2H) and its conjugate base, formate (HCO_2^-), are promising liquid hydrogen-storage media because of the low energy barrier to their formation from H_2 and CO_2 ($\Delta G^\circ_{298} = -4$ kJ mol^{-1})[5,14–19]. The equilibrium, given by

$$H_2\ (\text{aq.}) + CO_2\ (\text{aq.}) \rightleftharpoons HCO_2H\ (\text{aq.}) \qquad (1)$$

may therefore be viewed as a hydrogen storage system, with fuel-ready H_2 on the left-hand side, and stored H_2 on the right. Although formic acid fuel cells[20] and industrial processes that consume formic acid could be made more cost-effective by using reduced CO_2 as a C1 feedstock, we focus only on hydrogen storage in this study.

There has been excellent recent progress in developing catalysts targeted to either the reductive or oxidative components of hydrogen storage using formic acid, that is, in the separate steps for the hydrogenation of CO_2 and the decomposition of HCO_2H, respectively[15,21–43]. CO_2 hydrogenation has been achieved by Nozaki and colleagues using iridium pincer compounds, achieving rates as high as 150,000 h^{-1} at 200 °C and a turnover number (TON) of 3,500,000 at 120 °C (ref. 30). Langer and colleagues reported an iron pincer catalyst that operates at 156 h^{-1} and has a TON of 788 at 1 MPa and 80 °C (ref. 28). Meanwhile, Peris and colleagues have used alcohols in place of H_2 to obtain formate from CO_2 (refs 44–46). The high-pressure reduction of bicarbonate to formate has recently been used to reversibly store H_2 at 5–8 MPa and 70 °C (refs 31,47). The decomposition of formic acid is catalysed by numerous homogeneous and heterogeneous transition-metal compounds[4,21,22,34,38,48–51]. One of the present authors (Y.H.) has reported an iridium catalyst with a rate of 14,000 h^{-1} at 90 °C (ref. 22) and Boddien and colleagues have reported a TON of 92,000 with an iron catalyst at 80 °C (ref. 52). However, all reported high-turnover CO_2 hydrogenation catalysts require prohibitively high pressures and/or temperatures, often ranging from 5 to 6 MPa and 120 to 200 °C, respectively, and in some cases also requiring amine additives. Most importantly, no reported system, including metal-hydride and nanostructured materials, has been successful in reversibly storing H_2 in good yield within the same medium or under mild conditions.

Our approach to hydrogen storage using CO_2 and H_2 is shown in Fig. 1. A water-soluble, pH-modulated catalyst drives the hydrogenation of CO_2 to formate under basic conditions, and hydrogen release is easily triggered by acidifying the solution to protonate the catalyst. Progress has been reported in this regard (Y.H.) using well-defined pH-dependent catalysis with $[(Cp^*)Ir(dhbp)(OH_2)]SO_4$ ($[\mathbf{1(OH_2)}]SO_4$); dhbp = 4,4′-dihydroxy-2,2′-bipyridine; Cp* = pentamethylcyclopentadienide), which is activated once its 'multifunctional'[53] phenolic ligand is deprotonated[25]. The catalytic rate constant for this varies linearly with the ligand σ-donor power of the substituent on the phenanthroline or

[1]Chemistry Department, Brookhaven National Laboratory, Upton, New York 11973, USA, [2]National Institute of Advanced Industrial Science and Technology, Tsukuba Central 5-2, 1-1-1 Higashi, Tsukuba, Ibaraki 305-8565, Japan, [3]The Scripps Research Institute, 130 Scripps Way, Jupiter, Florida 33458, USA, [4]Department of Natural Science, Baruch College, CUNY, New York, New York 10010, USA. *e-mail: hull@bnl.gov; himeda.y@aist.go.jp; fujita@bnl.gov

© 2012 Macmillan Publishers Limited. All rights reserved.

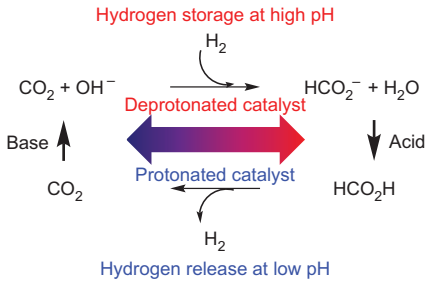

Figure 1 | Reversible H_2 storage is achieved by switching the pH to protonate or deprotonate the catalyst. H_2 is stored by the hydrogenation of CO_2 in the presence of hydroxide (basic aqueous conditions) and then regenerated by the addition of acid. The reductive (red) or oxidative (blue) reactions that interconvert CO_2, H_2 and HCO_2^-/HCO_2H can be favoured by protonating and deprotonating a proton-responsive catalyst.

bipyridine ligand backbone[22,24,25,53]. Because $\sigma^+_{p\,OH} = -0.91$ and $\sigma^+_{p\,O^-} = -2.30$, catalysis is greatly enhanced when the ligand is deprotonated to $-O^-$. Inspired by the use in nature of hydrogen bonds[54,55] and bases to relay protons in enzyme active sites[48,55], we sought to design a catalyst that would create synergy between electronic activation on the one hand, and the pendent-base properties of –OH or $-O^-$ on the other, as well as facilitate the interaction of H_2, CO_2, H_2O, HCO_2H, HCO_2^- and H^+ in the primary coordination sphere of iridium.

Here, we report the preparation and catalytic activity of $[\mathbf{2Cl_2}]^{2+}$ (Fig. 2a), a dinuclear Cp*Ir catalyst with 4,4′,6,6′-tetrahydroxy-2,2′-bipyrimidine (thbpym) as a bridging ligand. $[\mathbf{2Cl_2}]^{2+}$ crystallizes as the chloride salt, but rapidly hydrolyses to $[\mathbf{2(OH_2)_2}]^{4+}$ and $2Cl^-$ in water, and may then be deprotonated to $\mathbf{2'(OH_2)_2}$ above pH 5 (Fig. 2b). We observe superior catalytic performance using $\mathbf{2'(OH_2)_2}$ and $[\mathbf{2(OH_2)_2}]^{4+}$ for storing and releasing H_2, respectively, under very mild reaction conditions. For CO_2 hydrogenation,

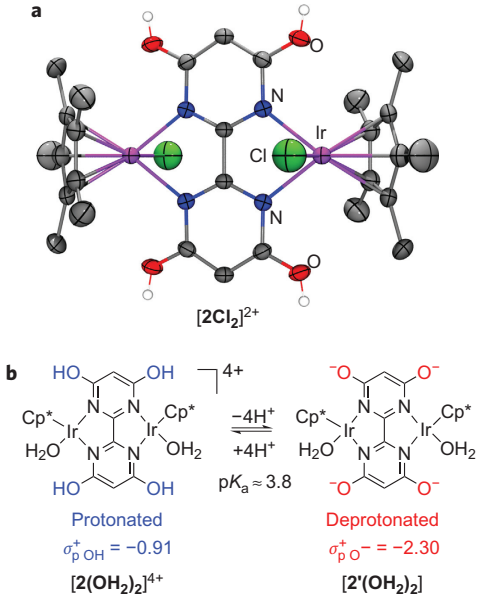

Figure 2 | Crystal structure of $2[Cl_2]^{2+}$ and reversible formation of $[\mathbf{2(OH_2)_2}]^{4+}$ and $\mathbf{2'(OH_2)_2}$. a, Thermal ellipsoid plot of **2** as $[\{Ir(Cp^*)(Cl)\}_2(thbpym)]^{2+}$, crystallized from aqueous Na_2SO_4. C–H bonds are omitted for clarity. **b**, Reversible formation of $[\mathbf{2(OH_2)_2}]^{4+}$ and $\mathbf{2'(OH_2)_2}$. The pendent –OH in $[\mathbf{2(OH_2)_2}]^{4+}$ is 'proton responsive' because it can be deprotonated to $-O^-$ to give $\mathbf{2'(OH_2)_2}$, where the ligand becomes a strong donor, as indicated by the Hammet parameter σ_p. $[\mathbf{2(OH_2)_2}]^{4+}$ and $\mathbf{2'(OH_2)_2}$ also have pendent bases close to the metal coordination sphere.

we observe high turnovers at room temperature and ambient pressure, and for the catalytic decomposition of formate the catalytic rate is faster than any previous report (228,000 h^{-1}). Accordingly, we have realized pH-switchable H_2 storage (as outlined in Fig. 1) with $\mathbf{2'(OH_2)_2}$ and $[\mathbf{2(OH_2)_2}]^{4+}$ for the first time. We are able to regenerate 2.3 MPa of H_2 following exposure of $\mathbf{2'(OH_2)_2}$ to 0.1 MPa of a 1:1 H_2:CO_2 mixture at room temperature, and then repeat the cycle. No CO gas impurities are detected, so the purity of the regenerated gas is suitable for use in some H_2 fuel cells, and the temperatures used are also well within fuel cell limits. To validate the role of thbpym in these reactions, we compared the catalytic activity of $[\mathbf{2(OH_2)_2}]^{4+}$ with the monometallic complex $[\mathbf{1(OH_2)}]^{2+}$ with activating groups but no pendent base, and with $[\mathbf{3Cl_2}]^{2+}$ ($[\{Ir(Cp^*)(Cl)\}_2(bpym)]^{2+}$, bpym = 2,2′-bipyrimidine), which has no activating groups or pendant bases.

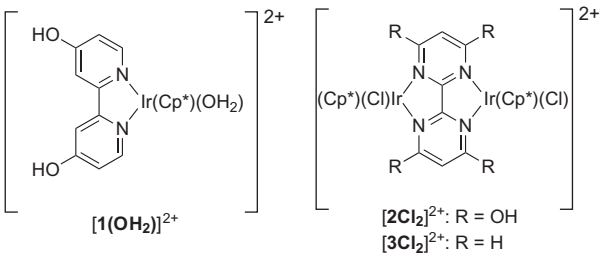

Our preliminary mechanistic studies and theoretical calculations support our hypothesis that the ligand –OH and $-O^-$ moieties significantly lower the energy barriers involved in H_2 storage via inner-sphere interactions with H_2 and HCO_2^-.

Results and discussion

Synthesis, structure and characterization of 2. The thbpym ligand was obtained by reducing 4,4′,6,6′-tetramethoxy-2,2′-bipyrimidine, and $[\mathbf{2Cl_2}]Cl_2$ was prepared by stirring a 1:1 mixture of $[Cp^*IrCl_2]_2$ and thbpym in methanol. Layering a methanolic solution of $[\mathbf{2Cl_2}]Cl_2$ onto concentrated Na_2SO_4 gave air-stable crystals suitable for X-ray diffraction (Fig. 2a). The crystal structure shows two iridium atoms, each coordinated to a Cp* ligand, a chloride ligand and to two nitrogen atoms of the bridging ligand to form a bimetallic complex. The Ir–N bond lengths are similar to those in $[\mathbf{3Cl_2}]^{2+}$, which was synthesized and compared to $[\mathbf{2Cl_2}]^{2+}$ because it is structurally similar but has no hydroxyl groups. Notably, the monometallic iridium catalyst could not be isolated when $[Cp^*IrCl_2]_2$ was used as the limiting reagent, suggesting that the affinity for the second iridium atom is high. The pK_a of the thbpym ligand was determined by an acid–base titration through $1 < pH < 13$ and a least-squares fit to determine the midpoint of the sigmoidal curve (Supplementary Fig. S1). The thbpym ligand in $[\mathbf{2(OH_2)_2}]^{4+}$ becomes deprotonated in the range $2 < pH < 5$ with a midpoint at pH 3.8 (ref. 56). Thus $pK_a = 3.8$ is an indication of the average acid dissociation constant for the thbpym ligand, and $[\mathbf{2(OH_2)_2}]^{4+}$ and $\mathbf{2'(OH_2)_2}$ exist in their fully protonated and deprotonated forms below pH 2 and above pH 5, respectively. The second midpoint near pH 9.8 (Supplementary Fig. S1 and ref. 56) is assigned to the ionization of $\mathbf{2'(OH_2)_2} \rightarrow [\mathbf{2'(OH)_2}]^{2-} + 2H^+$, indicating that this species is more basic than the aquo ligand in $\mathbf{1'(OH_2)}$ ($pK_a = 8.9$).

Catalytic hydrogenation of CO_2. The catalytic hydrogenation of CO_2 by iridium complexes $[\mathbf{1(OH_2)}]^{2+}$, $[\mathbf{2Cl_2}]^{2+}$ and $[\mathbf{3Cl_2}]^{2+}$ was investigated under a range of conditions (summarized in Table 1). Under the basic conditions investigated, $[\mathbf{1(OH_2)}]^{2+}$, $[\mathbf{2Cl_2}]^{2+}$ and $[\mathbf{3Cl_2}]^{2+}$ exist in water as $\mathbf{1'(OH_2)}$, $\mathbf{2'(OH_2)_2}$ and $[\mathbf{3(OH_2)_2}]^{4+}$, respectively, due to the rapid hydrolysis of Cl^-

© 2012 Macmillan Publishers Limited. All rights reserved.

Table 1 | Hydrogenation of CO_2 or bicarbonate (1 M $NaHCO_3$, pH = 8.4) in H_2O (1:1 H_2:CO_2).

Entry	Catalyst	Pressure (MPa)	Temp. (°C)	Initial TOF† (h^{-1})	TON	Final [formate] (M)	Ref.
1	$[RhCl(\eta^4C_8H_{12})]_2$	4	25	52	1,150	1.55	65
2	$RhCl(tppms)_3$	4	24	262	524	-	66
3	Ir(PNP)*	5‖	200	150,000	300,000	0.6	30
4	Ir(PNP)*	6‖	120	73,000	3,500,000	0.7	30
5	Ir(PNP′)*	5.5	185	14,500	348,000	0.7	27
6	**1′(OH$_2$)**	0.1	25	7	92	0.005	25
7	**2′(OH$_2$)$_2$**	0.1	25	64	7,200	0.36	Present
8	**2′(OH$_2$)$_2$**‡	0.1	25	70	2,230	0.56	Present
9	**2′(OH$_2$)$_2$**‡	4	50	15,700	153,000	1.53	Present
10	**2′(OH$_2$)$_2$**‡	5	80	53,800	79,000	0.16	Present
11	**2′(OH$_2$)$_2$**‡	3	50	9,400	42,500	1.70	Present
12	**2′(OH$_2$)$_2$**	1	50	3,050§	6,100	0.305	Present
13	**[3(OH$_2$)$_2$]$^{4+}$**	0.1	25	0	0	0	Present
14	**[3(OH$_2$)$_2$]$^{4+}$**	1	50	55§	110	0.006	Present

*PNP-type pincer ligand. †Averaged rate for initial 1 h. ‡Reaction carried out in 2 M $KHCO_3$. §Average rate for the entire reaction. ‖Total pressure at room temperature in 1 M KOH (5 ml) and THF (0.1 ml). See cited references for structures. These data, as well as catalyst concentration and reaction times, are shown in Supplementary Table S1.

(see Fig. 3). Entries 1–5 in Table 1 show selected results from other known systems, for comparison. However, good catalyst performance in those systems requires extraordinary pressures (above 5 MPa) and temperatures (120–200 °C). In contrast, when using a 1:1 H_2:CO_2 gas mixture at 0.1 MPa and 25 °C, **2′(OH$_2$)$_2$** achieved a turnover frequency (TOF) of 64 h^{-1} and TON of 7,200, and yielded 0.36 M formate (entry 7, pH 8.1). When 2 M $KHCO_3$ was used, the final formate concentration was increased to 0.56 M after 216 h and an initial TOF of 70 h^{-1} was achieved (Table 1, entry 8). This is an improvement of nearly an order of magnitude over our previous report of 7 h^{-1} for **1′(OH$_2$)** (entry 6), the only other catalyst that is active under ambient conditions (**1′(OH$_2$)** and **2′(OH$_2$)$_2$** are compared in Supplementary Fig. S2). The

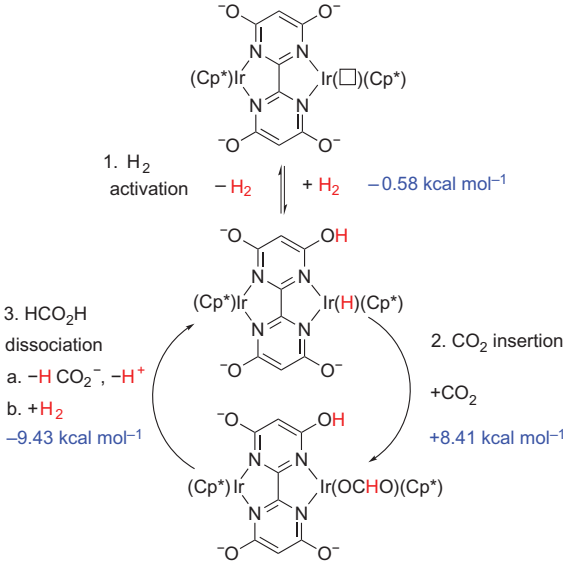

Figure 3 | Proposed mechanism and gas-phase free energy calculations for 2′(OH$_2$)$_2$ after it loses protons and water. (1) Activating H_2 and forming a metal hydride; (2) inserting CO_2 into the Ir–H bond; (3a) eliminating formate and a proton; and (3b) adding H_2 to regenerate the hydride. The free-energy changes in kcal mol^{-1} at pH 8.4 ($\Delta G^{\circ\prime}$) are indicated in blue. Only one iridium site is illustrated for clarity. See Supplementary Fig. S8 for the ^1H NMR spectrum of the Ir–H species, and Supplementary Figs S9 and S10 for theoretical details and the plotted free-energy surface. All energies are relative to the species indicated by an open square, which indicates a vacant coordination site, that is, after dissociation of the OH_2 or OH^- ligand.

reaction rate varies linearly with the concentration of **2′(OH$_2$)$_2$** (10–100 μM), indicating a first-order dependence (Supplementary Fig. S3). Rates and turnovers for **2′(OH$_2$)$_2$** were increased to a TOF of 53,800 h^{-1} and TON of 153,000 under pressurized conditions at relatively low temperature (Table 1, entries 9 and 10), resulting in a high concentration of 1.70 M formate solution (Table 1, entry 11). In comparison, **[3(OH$_2$)$_2$]$^{4+}$** shows no reaction at room temperature after 8 h (Table 1, entry 13), and only 110 turnovers under pressurized conditions (entry 14, T = 50 °C, P = 1 MPa, 2 h). The difference between the reaction rates of catalysts **2′(OH$_2$)$_2$** and **[3(OH$_2$)$_2$]$^{4+}$** clearly illustrates the effect of the ligand on the rate of catalytic CO_2 hydrogenation. Further investigations of the electronic effects that may contribute to this reaction are under way.

Retrieving H_2 from formic acid. Having established that **2′(OH$_2$)$_2$** efficiently converts CO_2 to aqueous formate under basic conditions, we examined the release of H_2 under acidic conditions. The results are summarized in Table 2. Under optimal reaction conditions (pH 3.5) the catalyst is intermediately protonated between **[2(OH$_2$)$_2$]$^{4+}$** and **2′(OH$_2$)$_2$**, and denoted **2*(OH$_2$)$_2$**. **2*(OH$_2$)$_2$** catalyses the release of H_2 and CO_2 (1:1) from aqueous HCO_2H/HCO_2Na mixtures at a TOF of 228,000 h^{-1} at 90 °C and TON of 308,000 at 80 °C, the highest TOF and TON yet reported (Table 2, entries 2 and 5). This performance is superior even to catalysts that require organic additives[35,42]. The liquid-to-gas conversion is quantitative in all cases, regardless of whether HCO_2H or HCO_2Na is used, although the latter is significantly slower (Supplementary Fig. S4.) Surprisingly, **[3(OH$_2$)$_2$]$^{4+}$** and **2*(OH$_2$)$_2$** generated H_2 from formate at similar rates at 60 °C (Table 2, entry 6). This suggests that the hydroxyl groups on the ligand have a larger effect in the hydrogenation of CO_2 than they do for the dehydrogenation of formic acid (see the mechanism in Fig. 3).

We also investigated the rate of H_2 evolution as a function of pH (Fig. 4). The rate peaks at 31,600 h^{-1} at pH 3.5, which is close to the pK_a of the catalyst (pK_a = 3.8) and to the pK_a of formic acid (pK_a = 3.75). These data, combined with the similar rates for **[3(OH$_2$)$_2$]$^{4+}$** and **2*(OH$_2$)$_2$**, suggest the ligands play different roles in the hydrogenation and dehydrogenation reactions. A thorough mechanistic investigation is under way.

pH-switchable consumption or production of H_2. Despite years of research, only two examples of reversible H_2 storage—that is, a system that starts with H_2, stores it, and subsequently regenerates H_2—have been reported. However, both systems required pressures of 8–10 MPa, and in one example the solvent had to be

© 2012 Macmillan Publishers Limited. All rights reserved.

Table 2 | Catalytic decomposition of HCO_2H by 1, 2 and 3.

Entry	Catalyst	Catalyst conc. (μM)	Temp. (°C)	Time (h)	Initial TOF† (h^{-1})	TON	Final [HCO_2H] (M)
1	$[\mathbf{1(OH_2)}]^{2+}$‡	200	60	4	2,400	5,000	0
2	$\mathbf{2^*(OH_2)_2}$‡	50	60	4	12,000	20,000	0
3	$\mathbf{2^*(OH_2)_2}$	50	60	18	31,600	16,800	0.16
4	$\mathbf{2^*(OH_2)_2}$	1.5	80	12	158,000	308,000	0.54
5	$\mathbf{2^*(OH_2)_2}$	3.1	90	7	228,000	165,000	0.48
6	$[\mathbf{3(OH_2)_2}]^{4+}$	50	60	1.5	32,000	10,000	0.50

Reaction conditions: 1 M HCO_2H/HCO_2Na (1:1, pH 3.5). †Averaged rate for initial 5–15 min. ‡1 M HCO_2H. $\mathbf{2^*(OH_2)_2}$ indicates that the thbpym ligand on **2** is intermediately protonated between $[\mathbf{2(OH_2)_2}]^{4+}$ and $\mathbf{2'(OH_2)_2}$ under the reaction conditions. See main text for details.

evaporated to reverse the reaction[31,47]. The proposal shown in Fig. 1 is unique, because pH, a well-defined and low-energy trigger, controls H_2 storage or production.

In a proof of concept study following Fig. 1, we exposed $\mathbf{2'(OH_2)_2}$ in 2 M $KHCO_3$ (20 ml) to a constant flow of a 1:1 CO_2:H_2 gas mixture at ambient pressure for 136 h to yield 0.48 M formate (Table 3, cycle 1). The reaction solution was then cooled and adjusted to pH 1.7 with 4 M sulfuric acid to protonate the catalyst to $[\mathbf{2(OH_2)_2}]^{4+}$. H_2 release was subsequently triggered by warming the solution in the glass autoclave to 50 °C, and resulted in a final closed-system pressure of 2.3 MPa of H_2/CO_2 (1:1), with no detectable CO by-product (Supplementary Fig. S5). Thus, pressure does not inhibit H_2 regeneration, an essential feature in using stored H_2 as a fuel[10]. The cycle was then repeated by cooling the system and adjusting the pH with $KHCO_3$. The system is therefore recyclable, and the catalyst does not need to be isolated before reuse. To our knowledge this is the first system—including metal organic frameworks, tank systems and other metal hydrides—that is capable of storing H_2 and creating a pressurized H_2 system under mild conditions[31,57]. Further efforts to optimize this storage process are ongoing. The exact experimental conditions are listed in the Supplementary Information, together with an additional scheme for the reaction cycle and a picture of the test vessel (Supplementary Figs S6 and S7, respectively).

Preliminary mechanism for CO_2 reduction. We hypothesized that introducing a ligand –OH moiety on $[\mathbf{2(OH_2)_2}]^{4+}$ would, via $\mathbf{2'(OH_2)_2}$, act as a base on an electronically activated catalyst. This is because H_2 would be activated by a proton relay[49,55], and because the Ir–H of $\mathbf{2'(H)_2}$ would be an excellent nucleophile for attack at CO_2 due to the high σ-donor power of the four $-O^-$ groups[15,27].

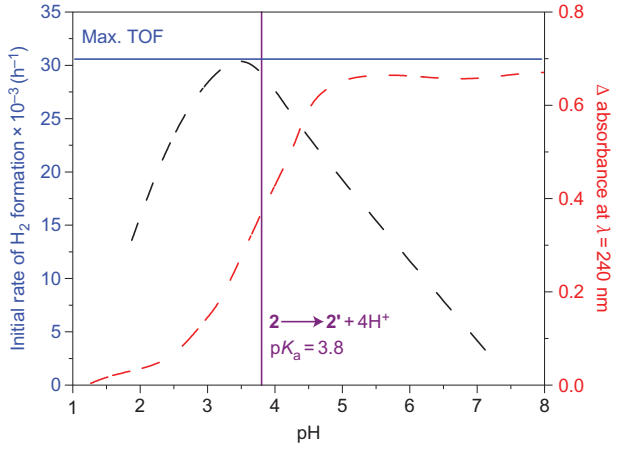

Figure 4 | Variation of the rate of H_2 evolution (left *y*-axis, blue) with pH compared to the ionization of the thbpym ligand (right *y*-axis, red). The mid-ionization point for $[\mathbf{2(OH_2)_2}]^{4+}$ to $\mathbf{2'(OH_2)_2}$ is indicated in purple, and the maximum TOF is shown in blue. See the main text for a discussion of this trend.

This is shown in steps 1 and 2 of Fig. 3. Our calculations and preliminary mechanistic experiments support this hypothesis, as does the experimentally determined absence of hydrogenation activity with $[\mathbf{3(OH_2)_2}]^{4+}$ described above. Water (or OH^-) replaces Cl^- as a ligand to iridium at a rate faster than could be measured by hand mixing experiments, and therefore $[\mathbf{3(OH_2)_2}]^{4+}$ is the starting complex before H_2 or CO_2 coordinate iridium.

An iridium hydride was easily formed experimentally with H_2 gas near room temperature and confirmed by the ^1H NMR singlet at −10.7 ppm in the ^1H NMR spectrum (Supplementary Fig. S8) by exposing $\mathbf{2'(OD_2)_2}$ to an atmosphere of H_2. A long T_1 relaxation time of 3,700 ms at 20 °C for the hydride singlet unambiguously indicates that a classical metal-hydride-type complex is formed in the presence of H_2 (ref. 58). Indeed, heterolytic cleavage of H_2 is known to be assisted by pendent bases in iridium complexes[55]. Bubbling H_2 through a solution of $\mathbf{2'(OH_2)_2}$ at basic pH caused shifts in the UV–visible spectrum from $\lambda_{max} = 335$ nm to $\lambda_{max} = 328$ nm at room temperature, followed by a shift to $\lambda_{max} = 342$ nm when CO_2 was bubbled through the same solution. These data are consistent with the standard mechanism for similar catalysts, which is (1) formation of an Ir–H species once H_2 displaces OH_2, followed by (2) insertion of CO_2 to give a formato complex, and (3) subsequent regeneration of the hydride with dissociation of formate or formic acid. Importantly, dissolved CO_2 was essential for formate production, and a very small amount of the product formed when only bicarbonate was used (Table 1). We therefore propose that CO_2 and not bicarbonate is reduced by $\mathbf{2'(OH_2)_2}$. The higher yield of formate in the presence of bicarbonate may therefore be due to the increased presence of dissolved CO_2, due to Le Chatelier's principle.

The calculated free energies of these intermediates adjusted for pH 8.4 in the gas phase are shown in Fig. 3, consistent with the experimental data in Table 1, and are plotted in Supplementary Fig. S10 (see Methods and Supplementary Information for theoretical details and energy tables). The formation of Ir–H in step 1 of Fig. 3 is slightly exoergic ($\Delta G^{\circ\prime} = -0.58$ kcal mol^{-1}), consistent with our proton-relay picture. Because pH 8.4 > catalyst pK_a, it is unlikely that the ligand remains protonated, and we cannot rule out the participation of bulk OH^- (ref. 59). The most endoergic step ($\Delta G^{\circ\prime} = +8.41$ kcal mol^{-1}) is CO_2 insertion into the Ir–H species (Fig. 3, step 2), seems rate limiting in these calculations

Table 3 | H_2 storage cycles according to Fig. 1.

Cycle	Hydrogenation of CO_2		Decomposition of formic acid		
	Time (h)	Generated formate (M)	Time (h)	Gas produced (MPa)	Formic acid remaining (M)
1	136	0.48	8	2.34	0.017
2	182	0.38	8	1.93	0.024

Hydrogenation reaction: $\mathbf{2'(OH_2)_2}$ dissolved in 2 M $KHCO_3$ under a constant flow of a 1:1 CO_2:H_2 at 0.1 MPa and 30 °C. Decomposition in a closed high-pressure vessel with $[\mathbf{2(OH_2)_2}]^{4+}$ at pH 1.7 and 50 °C. Experimental procedures are described in the Supplementary Information.

© 2012 Macmillan Publishers Limited. All rights reserved.

(supported by work by Fukuzumi and colleagues[60]). In contrast to Nozaki's and Hazari's catalysts[27,59,61], step 3 (displacing formate with H_2 to regenerate the Ir–H species) is moderately exoergic in our system ($\Delta G^{\circ\prime} = -9.43$ kcal mol^{-1}). The net $\Delta G^{\circ\prime}$ for the catalytic cycle is -1.60 kcal mol^{-1}, and the relatively flat free energy profile in this catalytic cycle may explain the superior catalytic activity of $\mathbf{2'(OH_2)_2}$ at room temperature. Although our calculations involve the reaction of only one of the iridium atoms, we expect that having two metal centres will increase the rate of catalysis[62]. Transition-state calculations for the consumption and production of H_2 will be presented in forthcoming work.

Summary and conclusion

We report the synthesis and characterization of $[\mathbf{2(OH_2)_2}]^{4+}$, the first catalyst capable of reversible H_2 storage using CO_2 in aqueous media under mild temperatures and pressures. A recyclable pressurization sequence demonstrates that low-pressure (atmospheric) H_2 gas can be stored as liquid formate, and then used to regenerate high-pressure H_2 and CO_2 for possible fuel applications. The –OH moieties on the thbpym ligand are pH-responsive, and H_2 storage can be turned on or off by adjusting the pH of the solution. CO_2 hydrogenation is facilitated because, in addition to electronically activating the catalyst, the $-O^-$ in $\mathbf{2'(OH_2)_2}$ facilitates H_2 heterolysis by acting as a pendent base. Rates as high as 70 h^{-1} (25 °C and 0.1 MPa) and 53,800 h^{-1} (80 °C and 5 MPa) are observed. $[\mathbf{2(OH_2)_2}]^{4+}$ decomposes formic acid or formate to give CO-free H_2 and CO_2 at low pH. We observe a TOF of 228,000 h^{-1} at 90 °C and TON of 308,000 at 80 °C, the highest TOF and TON yet reported. Detailed mechanistic and theoretical studies are in progress, as well as an investigation into H_2 formation from formate.

Methods

General. All manipulations were carried out under an argon atmosphere using standard Schlenk techniques or in a glovebox, and all aqueous solutions were degassed before use. ^{1}H NMR and ^{13}C NMR spectra were recorded on Varian INOVA 400 and Bruker Avance 400 and 500 spectrometers using sodium 3-(trimethylsilyl)-1-propanesulfonate (DSS sodium salt) as an internal standard. The X-ray structure was determined using a Bruker Kappa Apex II diffractometer. pH values were measured on an Orion 3-Star pH meter with a glass electrode after calibration to standard buffer solutions. The evolved gas was measured at various intervals by a gas meter (Shinagawa Corp., W-NK-05). H_2 was detected by a thermal conductivity detector using an activated 60/80 carbon column, and CO_2 and CO were detected using a flame ionization detector equipped with a methanizer using a Porapak Q 80/100 column at 50 °C on a GL Science GC390 gas chromatograph. Formate was produced from research-grade CO_2 (>99.999%) and H_2 (>99.9999%), or mixed gas ($CO_2/H_2 = 1/1$) through an O_2 trap. Formate product concentrations were monitored by high-performance liquid chromatography on an anion-exclusion column (Tosoh TSKgel SCX(H^+)) using aqueous H_3PO_4 solution (20 mM) as eluent and a ultraviolet detector ($\lambda = 210$ nm). $[Cp^*IrCl_2]_2$ was prepared by refluxing a suspension containing a 2:1 mixture of hydrated $IrCl_3$:Cp^* in methanol for 48 h (ref. 63). Complexes $[\mathbf{1(OH_2)}]^{2+}$ (ref. 24) and $[\mathbf{3Cl_2}]^{2+}$ (ref. 62) were prepared according to literature procedures. The synthetic procedures and characterization of the thbpym ligand and $[\mathbf{2Cl_2}]^{2+}$, as well as procedures for the uptake and regeneration reactions, are described in the Supplementary Information. Density functional theory calculations were performed using the Gaussian 09 software package[64] with the B3LYP functional and a CEP-121G basis set for iridium, and 6-31 + G(d,p) for C, N, O and H, and are described in detail in the Supplementary Information.

Received 22 September 2011; accepted 6 February 2012; published online 18 March 2012

References

1. Mikkelsen, M., Jorgensen, M. & Krebs, F. C. The teraton challenge. A review of fixation and transformation of carbon dioxide. *Energy Environ. Sci.* **3,** 43–81 (2010).
2. Arakawa, H. *et al.* Catalysis research of relevance to carbon management: progress, challenges, and opportunities. *Chem. Rev.* **101,** 953–996 (2001).
3. Sakakura, T., Choi, J. C. & Yasuda, H. Transformation of carbon dioxide. *Chem. Rev.* **107,** 2365–2387 (2007).
4. Fukuzumi, S. Bioinspired energy conversion systems for hydrogen production and storage. *Eur. J. Inorg. Chem.* 1351–1362 (2008).
5. Jessop, P. G., Joo, F. & Tai, C. C. Recent advances in the homogeneous hydrogenation of carbon dioxide. *Coord. Chem. Rev.* **248,** 2425–2442 (2004).
6. Morris, A. J., Meyer, G. J. & Fujita, E. Molecular approaches to the photocatalytic reduction of carbon dioxide for solar fuels. *Acc. Chem. Res.* **42,** 1983–1994 (2009).
7. Benson, E. E., Kubiak, C. P., Sathrum, A. J. & Smieja, J. M. Electrocatalytic and homogeneous approaches to conversion of CO_2 to liquid fuels. *Chem. Soc. Rev.* **38,** 89–99 (2009).
8. Doherty, M. D., Grills, D. C., Muckerman, J. T., Polyansky, D. E. & Fujita, E. Toward more efficient photochemical CO_2 reduction: use of $scCO_2$ or photogenerated hydrides. *Coord. Chem. Rev.* **254,** 2472–2482 (2010).
9. Jacobson, M. Z. Review of solutions to global warming, air pollution, and energy security. *Energy Environ. Sci.* **2,** 148–173 (2009).
10. Turner, J. A. Sustainable hydrogen production. *Science* **305,** 972–974 (2004).
11. Turner, J. A. A realizable renewable energy future. *Science* **285,** 687–689 (1999).
12. Schlapbach, L. & Zuttel, A. Hydrogen-storage materials for mobile applications. *Nature* **414,** 353–358 (2001).
13. Weidenthaler, C. & Felderhoff, M. Solid-state hydrogen storage for mobile applications: quo vadis? *Energy Environ. Sci.* **4,** 2495–2502 (2011).
14. Enthaler, S., von Langermann, J. & Schmidt, T. Carbon dioxide and formic acid—the couple for environmental-friendly hydrogen storage? *Energy Environ. Sci.* **3,** 1207–1217 (2010).
15. Himeda, Y. Conversion of CO_2 into formate by homogeneously catalyzed hydrogenation in water: tuning catalytic activity and water solubility through the acid–base equilibrium of the ligand. *Eur. J. Inorg. Chem.* 3927–3941 (2007).
16. Inoue, Y., Izumida, H., Sasaki, Y. & Hashimoto, H. Catalytic fixation of carbon dioxide to formic acid by transition metal complexes under mild conditions. *Chem. Lett.* 863–864 (1976).
17. Inoue, Y., Sasaki, Y. & Hashimoto, H. Synthesis of of formates from alcohols, carbon dioxide, and hydrogen catalyzed by a combination of group 8 transition metal complexes and tertiary amines. *J. Chem. Soc. Chem. Commun.* 718–719 (1975).
18. Jessop, P. G., Ikariya, T. & Noyori, R. Homogeneous hydrogenation of carbon dioxide. *Chem. Rev.* **95,** 259–272 (1995).
19. Jessop, P. G., Ikariya, T. & Noyori, R. Homogeneous catalytic-hydrogenation of supercritical carbon-dioxide. *Nature* **368,** 231–233 (1994).
20. Rice, C. *et al.* Direct formic acid fuel cells. *J. Power Source* **111,** 83–89 (2002).
21. Himeda, Y., Miyazawa, S. & Hirose, T. Interconversion between formic acid and H_2/CO_2 using rhodium and ruthenium catalysts for CO_2 fixation and H_2 storage. *ChemSusChem* **4,** 487–493 (2011).
22. Himeda, Y. Highly efficient hydrogen evolution by decomposition of formic acid using an iridium catalyst with 4,4′-dihydroxy-2,2′-bipyridine. *Green Chem.* **11,** 2018–2022 (2009).
23. Fellay, C., Dyson, P. J. & Laurenczy, G. A viable hydrogen-storage system based on selective formic acid decomposition with a ruthenium catalyst. *Angew. Chem. Int. Ed.* **47,** 3966–3968 (2008).
24. Himeda, Y. *et al.* pH-dependent catalytic activity and chemoselectivity in transfer hydrogenation catalyzed by iridium complex with 4,4′-dihydroxy-2,2′-bipyridine. *Chem. Eur. J.* **14,** 11076–11081 (2008).
25. Himeda, Y., Onozawa-Komatsuzaki, N., Sugihara, H. & Kasuga, K. Simultaneous tuning of activity and water solubility of complex catalysts by acid–base equilibrium of ligands for conversion of carbon dioxide. *Organometallics* **26,** 702–712 (2007).
26. Himeda, Y., Onozawa-Komatsuzaki, N., Sugihara, H., Arakawa, H. & Kasuga, K. Half-sandwich complexes with 4,7-dihydroxy-1,10-phenanthroline: water-soluble, highly efficient catalysts for hydrogenation of bicarbonate attributable to the generation of an oxyanion on the catalyst ligand. *Organometallics* **23,** 1480–1483 (2004).
27. Schmeier, T. J., Dobereiner, G. E., Crabtree, R. H. & Hazari, N. Secondary coordination sphere interactions facilitate the insertion step in an iridium(III) CO_2 reduction catalyst. *J. Am. Chem. Soc.* **133,** 9274–9277 (2011).
28. Langer, R. *et al.* Low-pressure hydrogenation of carbon dioxide catalyzed by an iron pincer complex exhibiting noble metal activity. *Angew. Chem. Int. Ed.* **50,** 9948–9952 (2011).
29. Fukuzumi, S., Kobayashi, T. & Suenobu, T. Efficient catalytic decomposition of formic acid for the selective generation of H_2 and H/D exchange with a water-soluble rhodium complex in aqueous solution. *ChemSusChem* **1,** 827–834 (2008).
30. Tanaka, R., Yamashita, M. & Nozaki, K. Catalytic hydrogenation of carbon dioxide using Ir(III)-pincer complexes. *J. Am. Chem. Soc.* **131,** 14168–14169 (2009).
31. Boddien, A. *et al.* CO_2'Neutral' hydrogen storage based on bicarbonates and formates. *Angew. Chem. Int. Ed.* **50,** 6411–6414 (2011).
32. Boddien, A. *et al.* Iron-catalyzed hydrogen production from formic acid. *J. Am. Chem. Soc.* **132,** 8924–8934 (2010).
33. Federsel, C. *et al.* A well-defined iron catalyst for the reduction of bicarbonates and carbon dioxide to formates, alkyl formates, and formamides. *Angew. Chem. Int. Ed.* **49,** 9777–9780 (2010).

© 2012 Macmillan Publishers Limited. All rights reserved.

34. Loges, B., Boddien, A., Gartner, F., Junge, H. & Beller, M. Catalytic generation of hydrogen from formic acid and its derivatives: useful hydrogen storage materials. *Top. Catal.* **53,** 902–914 (2010).
35. Boddien, A. *et al.* Continuous hydrogen generation from formic acid: highly active and stable ruthenium catalysts. *Adv. Synth. Catal.* **351,** 2517–2520 (2009).
36. Junge, H. *et al.* Improved hydrogen generation from formic acid. *Tetrahedron Lett.* **50,** 1603–1606 (2009).
37. Boddien, A. *et al.* Hydrogen storage in formic acid–amine adducts. *Chimia* **65,** 214–218 (2011).
38. Fukuzumi, S., Yamada, Y., Suenobu, T., Ohkubo, K. & Kotani, H. Catalytic mechanisms of hydrogen evolution with homogeneous and heterogeneous catalysts. *Energy Environ. Sci.* **4,** 2754–2766 (2011).
39. Urakawa, A., Jutz, F., Laurenczy, G. & Baiker, A. Carbon dioxide hydrogenation catalyzed by a ruthenium dihydride: a DFT and high-pressure spectroscopic investigation. *Chem. Eur. J.* **13,** 3886–3899 (2007).
40. Elek, J., Nadasdi, L., Papp, G., Laurenczy, G. & Joo, F. Homogeneous hydrogenation of carbon dioxide and bicarbonate in aqueous solution catalyzed by water-soluble ruthenium(II) phosphine complexes. *Appl. Catal. A* **255,** 59–67 (2003).
41. Laurenczy, G., Joo, F. & Nadasdi, L. Formation and characterization of water-soluble hydrido-ruthenium(II) complexes of 1,3,5-triaza-7-phosphaadamantane and their catalytic activity in hydrogenation of CO_2 and HCO_3^- in aqueous solution. *Inorg. Chem.* **39,** 5083–5088 (2000).
42. Morris, D. J., Clarkson, G. J. & Wills, M. Insights into hydrogen generation from formic acid using ruthenium complexes. *Organometallics* **28,** 4133–4140 (2009).
43. Tedsree, K. *et al.* Hydrogen production from formic acid decomposition at room temperature using a Ag–Pd core–shell nanocatalyst. *Nature Nanotech.* **6,** 302–307 (2011).
44. Azua, A., Sanz, S. & Peris, E. Water-soluble Ir-III *N*-heterocyclic carbene based catalysts for the reduction of CO_2 to formate by transfer hydrogenation and the deuteration of aryl amines in water. *Chem. Eur. J.* **17,** 3963–3967 (2011).
45. Sanz, S., Azua, A. & Peris, E. '(η^6-arene)Ru(bis-NHC)' complexes for the reduction of CO_2 to formate with hydrogen and by transfer hydrogenation with *i*PrOH. *Dalton Trans.* **39,** 6339–6343 (2010).
46. Sanz, S., Benitez, M. & Peris, E. A new approach to the reduction of carbon dioxide: CO_2 reduction to formate by transfer hydrogenation in iPrOH. *Organometallics* **29,** 275–277 (2010).
47. Papp, G., Csorba, J., Laurenczy, G. & Joó, F. A charge/discharge device for chemical hydrogen storage and generation. *Angew. Chem. Int. Ed.* **50,** 10433–10435 (2011).
48. DuBois, D. L. & Bullock, R. M. Molecular electrocatalysts for the oxidation of hydrogen and the production of hydrogen—the role of pendant amines as proton relays. *Eur. J. Inorg. Chem.* 1017–1027 (2011).
49. Dubois, M. R. & Dubois, D. L. Development of molecular electrocatalysts for CO_2 reduction and H_2 production/oxidation. *Acc. Chem. Res.* **42,** 1974–1982 (2009).
50. Yang, J. Y. *et al.* Mechanistic insights into catalytic H_2 oxidation by Ni complexes containing a diphosphine ligand with a positioned amine base. *J. Am. Chem. Soc.* **131,** 5935–5945 (2009).
51. DuBois, M. R. & DuBois, D. L. The role of pendant bases in molecular catalysts for H_2 oxidation and production. *C. R. Chim.* **11,** 805–817 (2008).
52. Boddien, A. *et al.* Efficient dehydrogenation of formic acid using an iron catalyst. *Science* **333,** 1733–1736 (2011).
53. Crabtree, R. H. Multifunctional ligands in transition metal catalysis. *New J. Chem.* **35,** 18–23 (2011).
54. Dobereiner, G. E. *et al.* Iridium-catalyzed hydrogenation of *N*-heterocyclic compounds under mild conditions by an outer-sphere pathway. *J. Am. Chem. Soc.* **133,** 7547–7562 (2011).
55. Lee, D. H., Patel, B. P., Clot, E., Eisenstein, O. & Crabtree, R. H. Heterolytic dihydrogen activation in an iridium complex with a pendant basic group. *Chem. Commun.* 297–298 (1999).
56. Dixon, H. B. F. Relations between the dissociation-constants of dibasic acids. *Biochem. J.* **253,** 911–913 (1988).
57. Leitner, W., Dinjus, E. & Gaßner, F. Activation of carbon dioxide: IV. Rhodium-catalysed hydrogenation of carbon dioxide to formic acid. *J. Organomet. Chem.* **475,** 257–266 (1994).
58. Crabtree, R. H., Segmuller, B. E. & Uriarte, R. J. T1s and proton NMR integration in metal hydride complexes. *Inorg. Chem.* **24,** 1949–1950 (1985).
59. Yang, X. Z. Hydrogenation of carbon dioxide catalyzed by PNP pincer iridium, iron, and cobalt complexes: a computational design of base metal catalysts. *ACS Catal.* **1,** 849–854 (2011).
60. Ogo, S., Kabe, R., Hayashi, H., Harada, R. & Fukuzumi, S. Mechanistic investigation of CO_2 hydrogenation by Ru(II) and Ir(III) aqua complexes under acidic conditions: two catalytic systems differing in the nature of the rate determining step. *Dalton Trans.* 4657–4663 (2006).
61. Ahlquist, M. S. G. Iridium catalyzed hydrogenation of CO_2 under basic conditions—mechanistic insight from theory. *J. Mol. Catal. A* **324,** 3–8 (2010).
62. Govindaswamy, P. *et al.* Mono and dinuclear rhodium, iridium and ruthenium complexes containing chelating 2,2′-bipyrimidine ligands: synthesis, molecular structure, electrochemistry and catalytic properties. *J. Organomet. Chem.* **692,** 3664–3675 (2007).
63. White, C., Yates, A., Maitlis, P. M. & Heinekey, D. M. *(η^5-Pentamethylcyclopentadienyl)Rhodium and -Iridium Compounds* (Wiley, 2007).
64. Gaussian 09 RevB.01, Gaussian Inc., Wallingford, CT.
65. Graf, E. & Leitner, W. Direct formation of formic-acid from carbon dioxide and dihidrogen using the $(Rh(COD)Cl)_2$ $Ph_2P(CH_2)_4PPh_2$ catalyst system. *J. Chem. Soc. Chem. Commun.* 623–624 (1992).
66. Joo, F., Laurenczy, G., Nadasdi, L. & Elek, J. Homogeneous hydrogenation of aqueous hydrogen carbonate to formate under exceedingly mild conditions—a novel possibility of carbon dioxide activation. *Chem. Commun.* 971–972 (1999).

Acknowledgements

The work at Brookhaven National Laboratory is funded under contract DE-AC02-98CH10886 with the US Department of Energy and supported by its Division of Chemical Sciences, Geosciences, & Biosciences, Office of Basic Energy Sciences. J.F.H. acknowledges support as a BNL Goldhaber Distinguished Fellow. Y.H. acknowledges support from the Japanese Ministry of Economy, Trade, and Industry. R.P. and B.H. were supported by the CCHF 101 (grant no. DE-SC0001298).

Author contributions

J.F.H. and Y.H. conceived the project, carried out the bulk of the experimental work and wrote the manuscript. W.W. made significant contributions to the synthesis and characterization. R.P. and B.H. provided the thbpym ligand. D.J.S. solved the crystal structure. J.T.M. carried out theoretical work and E.F. oversaw all work.

Additional information

The authors declare no competing financial interests. Supplementary information and chemical compound information accompany this paper at www.nature.com/naturechemistry. Reprints and permission information is available online at http://www.nature.com/reprints. Correspondence and requests for materials should be addressed to J.F.H., Y.H. and E.F.

© 2012 Macmillan Publishers Limited. All rights reserved.